ON STEADY STATE AND DYNAMIC PERFORMANCE OF MODEL REFERENCE CONTROL FOR A PERMANENT MAGNET SYNCHRONOUS MOTOR.

Paul Stewart and Visakan Kadirkamanathan. Department of Automatic Control and Systems Engineering. University of Sheffield. U.K.

Keywords: Automotive systems, non-linear systems, multivariable control systems.

1. ABSTRACT.

Due to high power density and efficiency, permanent magnet AC motors are becoming the machines of choice for industrial and vehicle drive applications.
The useful speed range of the permanent magnet motor can be extended many times past its nominal base speed by advancing the phase of the applied three phase sinusoidal currents. The relationship between torque output, angular velocity and current phase advance is multivariable and non-linear in this extended speed range. Other non-linearities are due to the switching effects of the PWM current controllers.
Time varying parameters such as battery supply voltage in traction applications and inductance variation due to temperature are significant, consequently robustness is an important criteria of controller design, as is the optimal placement of the current vector at all times in order to make the most efficient use of available energy sources. This is particularly important for traction applications which require the most efficient use of available battery reserves.
Existing control strategies seldom explore the dynamic system characteristics, relying upon the onset of current errors to detect and regulate current phase advance. Also, look-up table functions are the solution of steady state equations. For high performance motors with small time constants, insufficient voltage headroom is available at the onset of current error to allow movement of the current vector to its optimal position quickly enough, with resulting reduced torque output or instability.
A model reference control method is proposed, which has a relatively small computational overhead, forms an appropriate basis for adaptive methods, and controls the system smoothly through the transition into the phase advance mode by extending the controller to utilise the dynamic system terms. The onset of phase advance is anticipated, the resulting voltage headroom allowing the model reference to retain control of the current vector.

2.BACKGROUND.

The control techniques for motor control below base speed have been available for some time. Jahns [1] presents the motor inverter topology necessary to achieve sinusoidal shaping of the applied current with control available over current magnitude, frequency and phase. A PWM current control algorithm is applied to eliminate all major low order harmonics of the excitation waveforms. A variety of PWM algorithms exist to perform the sinusoidal waveshaping Enjeti et.al [2], Brod et. al.[3].

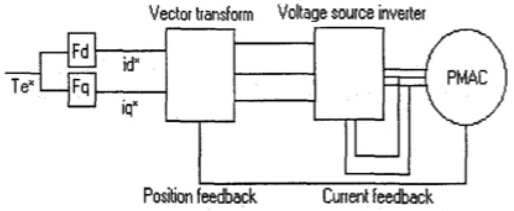

Figure 1 Maximum torque per amp controller.

The baseline approach adopted by Jahns achieves maximum torque per amp operation below base speed, illustrated in figure 1.
The torque demand T_e^* is mapped into d and q-axis commands by the functions F_d and F_q respectively. The current commands in the d-q reference frame are then transformed into instantaneous sinusoidal reference phase current commands by the vector transform block, using rotor angle feedback.
The functions F_d and F_q determined under steady state conditions, represent maximum torque per amp look-up tables which supply commands to d and q-axis PID current controllers.
In an earlier paper Jahns [4], presents a method of flux weakening a salient pole motor. The algorithm is an extension to the method previously described in [1], using current feedback to identify the onset of current regulator saturation. Saturation is identified by the onset of d axis current error. This method is illustrated in figure 2.
The action of the flux weakening algorithm is to depress the q-axis current command i_q^* when current regulator saturation is detected via the presence of d-axis error. By limiting the maximum value of i_q^*, the current command vector i_s^* which initially lies outside the voltage limit ellipse is forced back into the ellipse (for a salient pole machine).
The method is a simple one, the function blocks must be implemented as explicit look-up tables which have been derived analytically beforehand. This controller method can become expensive in terms of processor memory, and is also relatively inflexible. Although convergence to a solution is achievable in the field weakening region, it relies to a large extent on the time constant of the

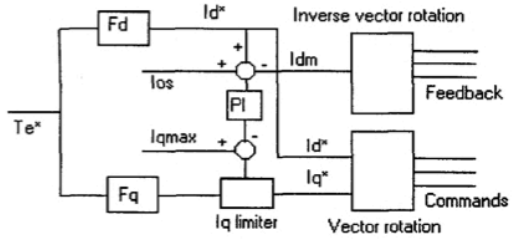

Figure 2 Field weakening controller for a salient pole motor.

motor. Also, it is uncertain that the solution is optimal in terms of efficiency or performance.

Morimoto [5] and Jahns [6] extend the flux weakening feedforward controller by adding functions which reflect the explicit solution of the steady state PMSM system equations. As in figure 2, functions control the system below base speed to follow the maximum torque per amp trajectory. Above base speed, the current vector is forced to intersect with the boundary of the voltage limit circle. At any given speed, bus voltage and i_d^* value, the controller limits i_q^* to a maximum attainable value given by;

$$i_{q\max} = \sqrt{\left(\frac{V_o}{X_q}\right)^2 - \left(\frac{X_d}{X_q}\right)^2 \left[i_d^* + \frac{\omega_e \psi_{mag}}{X_d}\right]^2} \qquad (1)$$

The controller operates the motor at the maximum attainable torque per stator current amp in the presence of current regulator saturation. However since the controller operates by limiting the i_q demand, and moving the i_d demand along the voltage limit circle/ellipse, there exist reservations. Again the controller relies on system time constant, and takes a finite time to converge to a solution. Also the algorithm does not address the problem of operating the motor in the flux weakening region but below maximum torque, where the current regulators are not saturated, and multiple solutions of the system equations exist. In order to introduce some measure of robustness, this method relies upon knowledge of the lowest expected value of supply voltage. In vehicle drive applications, the battery voltage can be expected to vary between maximum nominal Volts and zero Volts. Hence this method falls short of the performance required.

The feedforward controller is developed further by Kim and Sul [7]. The scheme is illustrated in figure 3.

The torque producing capability in the flux weakening region is determined by the machine current and voltage limits. In this region, the maximum torque output is produced by d-q current values corresponding to the intersection of the current and voltage limit circles. The onset of current regulator saturation varies according to

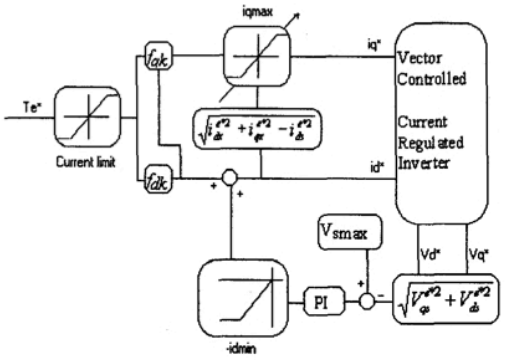

Figure 3 Feedforward field weakening controller.

load condition and machine parameters. Late onset of flux weakening results in an undesirable output torque drop, too early an onset degrades the machines ability to accelerate.

In the above scheme, functions f_{qk} and f_{dk} control the machine in the constant torque region, with the current vector lying on the maximum torque per amp trajectory until the current regulators begin to saturate.

The adjustable i_{qmax} function depresses the q-axis current command in response to the growing d-axis current demand. The function i_{dmin} forces the current vector to converge to a solution along the voltage circle ellipse.

The methods presented make no reference to the minimisation of the magnitude of the current vector in unsaturated conditions, or to the issue of parameter variations. For high performance applications, the time constant of the machine may by necessity be very short. This makes severe demands of the controller, and may preclude the use of controllers which need a relatively long time for convergence.

The proposed controller design implements a model reference which supplies optimal command signals under all operating conditions, minimising the magnitude of the current vector at all times without recourse to convergence to a solution.

3.THE PERMANENT MAGNET AC MOTOR.

The permanent magnet AC motor under consideration has magnets surface mounted onto a circular cross-section shaft. For this topology, the d and q-axis synchronous reactances are equal.

The stator currents are transformed into an orthogonal frame of reference which is moving synchronously with the rotor flux. The orthogonal reference frame (with axes d and q) is derived from the phase currents via the Park transform (Kim et.al)[7];

$$\begin{vmatrix} i_{dk} \\ i_{qk} \end{vmatrix} = \frac{2}{3} \begin{vmatrix} \sin\theta_r & \sin(\theta_r - 120^0) & \sin(\theta_r + 120^0) \\ \cos\theta_r & \cos(\theta_r - 120^0) & \cos(\theta + 120^0) \end{vmatrix} \begin{vmatrix} i_a \\ i_b \\ i_c \end{vmatrix} \qquad (2)$$

Since the motor has a sinusoidal back-emf and assuming negligible effects from magnetic saturation, then the d and q-axis voltage equations may be expressed thus [7];

$$V_{qs}^{*} = r_s i_{qs}^{*} + \omega_r \left(L_s i_{ds}^{*} + \lambda_m \right) + L_s \frac{di_{qs}^{*}}{dt} \quad (3)$$

$$V_{ds}^{*} = r_s i_{ds}^{*} - \omega_r L_s i_{qs}^{*} + L_s \frac{di_{ds}^{*}}{dt} \quad (4)$$

The expression for instantaneous torque is [7];

$$T_e = \frac{3P}{2} \phi_f i_q = k_t i_q \quad (5)$$

It can be seen that the back-emf term ($\omega\lambda$) increases linearly with rotor velocity and opposes the torque producing component i_q. Also, the maximum torque per amp operating condition is achieved by controlling the d-axis current to zero, allowing the current vector to be aligned in the direction of the q axis. If i_d is controlled to zero, then rotor velocity can increase to a frequency limited by the supply voltage, above which the torque producing component declines rapidly. The rotor is said to have attained "base speed" at the point where the magnitude of the back-emf equals the supply voltage, and torque production is zero.

If at this point, negative d-axis current can be introduced, countering the back-emf, the speed range of the motor can be extended albeit at lower levels of maximum torque.

The open circuit emf (E_q) is a sinewave lagging the magnet flux by 90 degrees. The voltage drop across the synchronous reactance is jX_sI and leads the current phasor by 90 electrical degrees.

The applied terminal voltage must equal the sum of the back-emf and voltage drop phasors.

When the current and voltages are resolved into d and q-axis components, the mechanism of phase advance in the field weakening region can be illustrated for any velocity and phase advance as in figure 4. Since the maximum magnitude of the voltage vector V is fixed by the link voltage, negative d-axis current is injected to achieve extended speed operation at the cost of reduced torque.

4. STEADY STATE CONDITIONS AND MODEL REFERENCE.

The maximum current that can be supplied to the motor is limited by the heat dispersion properties of the motor and the current rating of the inverter. It is also limited by the dc link voltage which must equal the back-emf and the voltage drops across the resistance and synchronous reactance.

In the orthogonal reference plane, the current limit I_c is a circular locus (6);

$$I^2{}_c = I_d^2 + I_q^2 \quad (6)$$

The maximum voltage V_c is also a circular locus with radius given by (7) [7]:

$$V_d^2 + V_q^2 = V_c^2 \quad (7)$$

thus;

$$X_s^2 I_q^2 + \left(E_q + X_s I_d \right)^2 = V_c^2 \quad (8)$$

and;

$$I_q^2 + \left[I_d + \frac{E_q}{X_s} \right]^2 = \frac{V_c^2}{X_s^2} \quad (9)$$

Equations 6-9 are represented in phasor diagram figure 4, which is the solution of the steady state equations for a 76kW permanent magnet AC synchronous machine produced by MST Ltd. Sheffield U.K. The electrical data is as follows;

Phase self inductance: 118µH.
Phase mutual inductance: 59 µH.
Phase resistance @ 25° C : 2.46 mΩ.
Pole number: 8.
Torque constant: 0.48 Nm/A_{rms}
Phase emf constant: 0.26 V/rad/s

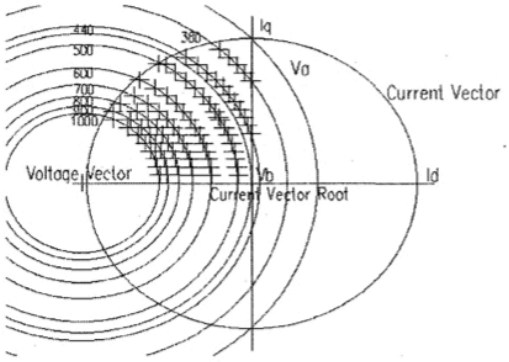

Figure 4 Experimental motor optimal phase advance map.

The motor gives a nominal peak torque of 170 Nm to base speed at 354A limit, and a peak power profile of 76kW to the top speed of 10,000 rpm.

The system equations were solved numerically for a set of torque speed combinations covering the whole operating envelope of the motor, within the constraint of minimising the magnitude of the current vector at all times.

Since the vector map in figure 4 represents the optimal solution to the minimum current vector criteria, it is possible to use this vector map as the basis for a model reference control system.

The principle of the model reference controller is illustrated in figure 5. Based on velocity and current feedback, the model reference controller outputs d and q-axis commands into separate d and q-axis PID

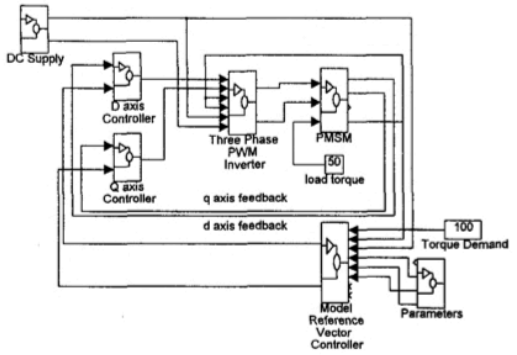

Figure 5 PMSM model reference controller simulink model.

controllers which drive the current error components to zero.

The controller calculates the frequency vector root position from (9) [7] as;

$$\left(-\frac{E_q}{X_s},0\right) \tag{10}$$

Also from (9), a frequency vector F magnitude is calculated as;

$$F=\left(\frac{V_c}{X_s}\right) \tag{11}$$

A torque demand vector magnitude T is calculated from the frequency vector root as;

$$T=\sqrt{F^2+i_q^{*2}} \tag{12}$$

The model reference controller has three modes of operation as follows;

1.The frequency vector F has a greater magnitude than the torque demand vector T. This mode corresponds to constant torque operation below base speed. The q-axis request is passed on as the q-axis command, and the d-axis command is zero (figure 6).

2.The frequency vector F has a smaller magnitude than the torque vector T, and the torque demand is achievable, with multiple solutions for i_d (figure 7). The controller calculates the intersection of the torque demand level with the frequency circle, and the appropriate value of d-axis command.

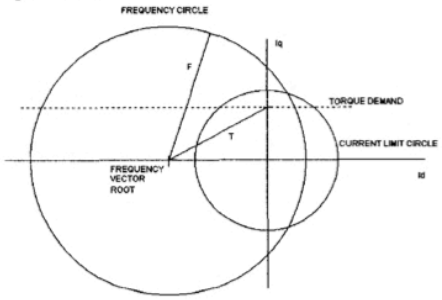

Figure 6 Model reference mode 1.

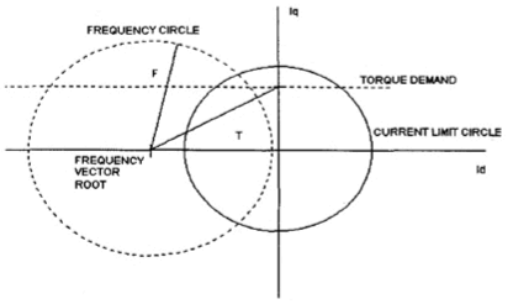

Figure 7 Model reference mode 2.

3.The frequency vector magnitude F is smaller than the magnitude of the torque vector T. However, the requested level of torque is not available (figure 8). The model reference calculates the highest available torque value, which corresponds with the intersection of the maximum current and frequency circles. The appropriate d and q-axis commands are then generated.

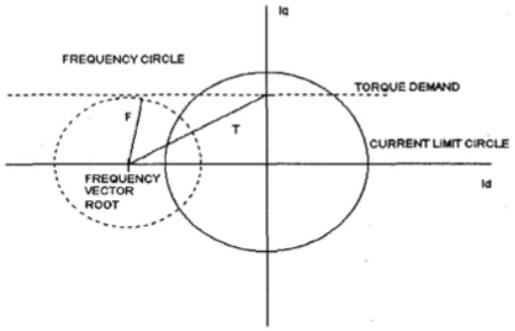

Figure 8 Model reference mode 3.

Rather than using a fixed multi-dimensional lookup-table, the reference model is implemented as a geometrical solution, which facilitates the implementation of parameter estimation and makes smaller demands on DSP memory.

5.STEADY STATE CONTROLLER.

The model reference controller, three phase PWM inverter and permanent magnet synchronous motor were implemented in Simulink. Position information was simulated as an absolute 12-bit encoder, and for initial simulations, current and voltage feedback signals were not corrupted by noise.

The simulation was run in steady state conditions, in order to correlate its results with a set of steady state experimental results carried out on a dynamometer test rig. A full range of torque demands (per unit) were made through the entire speed range of the motor, the results are presented in figures 9 and 10.

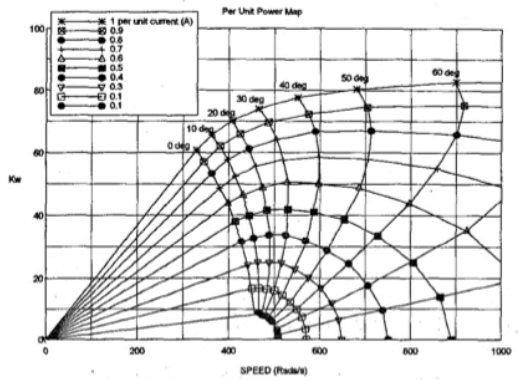

Figure 9 Experimental motor steady state per-unit power map.

The per unit torque output is shown as a function of current vector advance angle and rotor velocity. The simulation results matched the steady state experimental results obtained from the dynamometer confirming the accuracy of the controller and motor drive model.

Although the steady-state performance is a useful indicator of the accuracy of the motor model, the drive system is governed by the dynamic equations (3),(4). Since the model reference controller is based upon steady-state analysis, it was anticipated that the unmodelled dynamics would cause degradation in system performance. This effect is a function of the unmodelled voltage drop due to the dynamic operation of the system. Figure 11 illustrates the effects of these dynamics.

The upper series is the maximum torque envelope in steady state (current limit set to 354 A). The middle series is the dynamic envelope of the system controlled by the steady state model reference, and the lower series is the measured voltage drop due to unmodelled dynamics.

The steady state model reference controller was found to be useable, and relatively simple to implement. However, by extending the model reference to full dynamic capability, improvements can be made to the torque speed response.

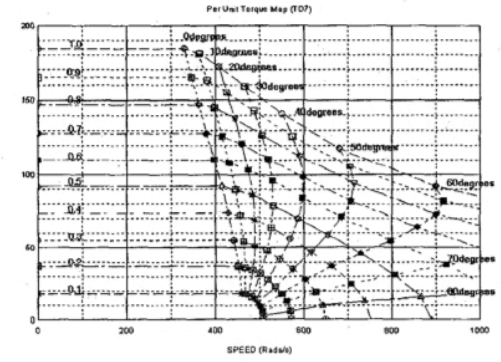

Figure 10 Experimental motor per-unit torque map.

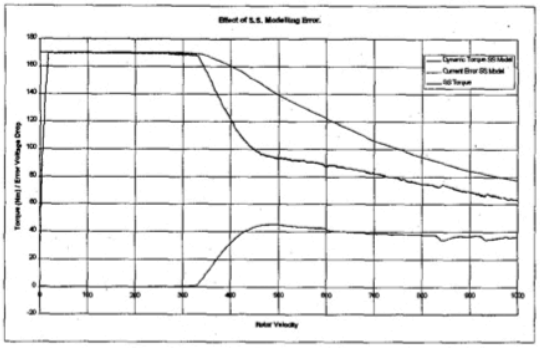

Figure 11 Steady state model reference controller response.

6.DYNAMIC MODEL REFERENCE CONTROLLER.

Since the system can be described as a series of balanced voltage drops, applied voltage and back emf, two expressions can be formed from (3) and (4);

$$V_{qs}^{*} = V_{qsteadystate} + L_s \frac{di_q}{dt} \tag{13}$$

$$V_{ds}^{*} = V_{dsteadystate} + L_s \frac{di_d}{dt} \tag{14}$$

This implies that a voltage drop exists due to the rate of change of current vector advance angle. Thus the controller can be extended by introducing the term;

$$V_{cdynamic} = V_s - \sqrt{\left(L_s i_q \frac{d\theta}{dt}\right)^2 + \left(L_s i_d \frac{d\theta}{dt}\right)^2} \tag{15}$$

Where θ is the angle of current vector advance. From (3) and (4) the following equation can be derived;

$$\frac{d\theta}{dt} = \frac{k_t \left[L^2 I^2 + 2LI \sin(\theta)\lambda_s + \lambda_s{}^2\right]}{w\lambda_s LJ} \tag{16}$$

In order to reserve sufficient voltage headroom to allow the current vector dynamics, a new lower base speed is calculated to switch in compensation (15).

Figure 12 compares the steady state controller and dynamic controller, all operating at a nominal dc link voltage of 240V. The magnitude of voltage drop due to dynamic effects and the rotor velocity at which this occurs is estimated by the dynamic module.

A dramatic improvement in the torque envelope is observed which benefits rotor acceleration.

The dynamic controller provides improved performance over the steady state method, with the current remaining under control at all times. This is due to the controller maintaining the inverter operation just below voltage saturation.

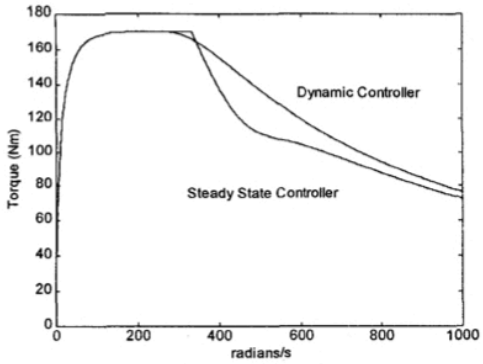

Figure 12. Model reference controller comparison.

7. CONCLUSION AND FUTURE WORK.

A full dynamic controller for permanent magnet AC machines has been designed and simulated. The steady-state performance has been verified experimentally. The controller fulfills the design criteria of four quadrant operation with optimal power usage. The controller allows a relatively simple implementation on a DSP, embodying as much *a priori* knowledge as possible.

The dynamic simulation results will be verified experimentally, and the controller extended to include parameter variation estimation. A self comissioning module will be added to make the initial parameter estimates.

Certain specifications require that position information be supplied by a brushless DC optical encoder with a resolution of only 120° electrical, which will necessitate position estimation.

The drive system is to form a unit with an electronic gearbox, which requires velocity synchronisation, possibly within an electrical cycle.

Future work will necessitate the use of intelligent methods to gain the required levels of performance.

REFERENCES.

[1] Thomas M. Jahns. 1994. "Motion control with permanent magnet AC machines." Proc. IEEE, Vol. 82, No. 8, pp1241-1252

[2] P.N. Enjeti, P.D. Ziogas, J.L. Lindsay. 1990. "Programmed PWM techniques to eliminate harmonics: a critical evaluation." IEEE Trans. Ind. App., Vol. 26, No. 2, pp302-316

[3] D.N. Brod, D.W. Novotny. 1985. "Current control of VSI - PWM inverters.". IEEE Trans. Ind.App., Vol. 1A-21, No.3. pp562-570

[4] Thomas M. Jahns. 1987. "Flux-weakening regime operation of an interior permanent magnet synchronous motor drive.". IEEE Trans. Ind. App., Vol. 1A-23, No. 4, pp681-689

[5] S. Morimoto 1994. "Wide speed operation of interior permanent magnet synchronous motors with high performance current regulator.". IEEE Trans. Ind. App., Vol. 30, No. 4., pp920-926

[6] S.R.Macminn, Thomas M. Jahns. 1991. "Control techniques for improved high speed performance of interior permanent magnet synchronous motor drives." IEEE Trans. Ind. App., Vol. 27, No. 5, pp997-1004

[7] J. M. Kim, S. K. Sul 1997. "Speed control of interior permanent magnet synchronous motor drive for the flux weakening operation.". IEEE Trans. Ind. App., Vol. 33, No. 1, pp43-48

8. GLOSSARY.

$i_d^*, i_{ds}^{e*}, i_q^*, i_{qs}^{e*}$	d and q-axis commands
i_{ds}, i_{qs}	d and q-axis currents
i_a, i_b, i_c	phase currents
i_{qmax}	q-axis current limit
i_s^*	current vector command
V_o	voltage vector
X_d, X_q	d and q-axis synchronous reactance
ω_e, ω_r	rotor angular velocity
φ_{mag}	flux linkage
V_{smax}	Voltage limit
i_{dmin}	d-axis current limit
$V_{qs}^{e*}, V_{ds}^{e*}, V_{qs}^*, V_{ds}^*, V_d^*, V_q^*$	d and q-axis voltage commands
θ_r	rotor position
r_s	phase resistance
L_s	phase inductance
λ_s	back-emf constant
T_e	instantaneous torque
P	pole pairs
ϕ_f	flux
k_t	torque constant
i_q, i_d	d and q-axis currents
I_c	current limit
V_q	q-axis voltage
V_d	d-axis voltage
V_c	voltage limit
E_q	back-emf constant